



ISSN: 2230-9926

Available online at <http://www.journalijdr.com>

IJDR

International Journal of Development Research

Vol. 12, Issue, 05, pp. 55901-55906, May, 2022

<https://doi.org/10.37118/ijdr.24425.05.2022>



RESEARCH ARTICLE

OPEN ACCESS

PERFORMANCE OF CERAMIC TILES APPLIED IN STRUCTURAL MASONRY MODEL USING ACTIVE THERMOGRAPHY

Fabiola M. M. P.Nunes¹, Cristiane B. C. S. Alvarenga¹, Rosemary B. C. Sales^{2,*}, Maria Teresa P. Aguilar¹ and Antônio N. Carvalho Júnior¹

¹Department of Materials Engineering and Construction, Federal University of Minas Gerais, Brazil 30000-000,

²Department of Planning and Configuration, Minas Gerais State University, Brazil 30000-000

ARTICLE INFO

Article History:

Received 27th February, 2022

Received in revised form

08th March, 2022

Accepted 19th April, 2022

Published online 20th May, 2022

Key Words:

Facades, Pathologies,
Ceramic Tiles,
Active Infrared Thermography.

ABSTRACT

The use of ceramic tiles on facades is a common practice in certain regions/countries. It is justified by its aesthetic functions and by the increase in the useful life of buildings. However, it is considered a complex system as it involves different technical components(blocks, Roughcast, Plaster, ceramic tiles and grouting). Considering that cladding introduces an additional barrier to the passage of heat, it is expected that its use promotes a greater thermal comfort in the built environment. Studies have evaluated facades tiles cladding using infrared thermography (IRT). However, there are few studies on the influence of cladding on the thermal comfort of buildings, especially assessed by IRT. In this study, the performance of models consisting of structural masonry of cladded red ceramic blocks is evaluated by active IRT. The results of temperature analysis obtained 60 minutes after heating indicate that plaster and ceramic tiles play an important role in facades, what it could contribute to thermal comfort. The contribution of ceramic tiles is greater than that of plaster.

*Corresponding author:

Rosemary B. C. Sales

Copyright © 2022, Fabiola M. M. P.Nunes et al. This is an open access article distributed under the Creative Commons Attribution License, which permits unrestricted use, distribution, and reproduction in any medium, provided the original work is properly cited.

Citation: Fabiola M. M. P.Nunes, Cristiane B. C. S.Alvarenga, Rosemary B. C. Sales, Maria Teresa P. Aguilar¹ and Antônio N. Carvalho Júnior. "Performance of ceramic tiles applied in structural masonry model using active thermography", *International Journal of Development Research*, 12, (05), 55901-55906.

INTRODUCTION

Ceramic tiles materials are widely used for cladding facades. In addition to the aesthetic function, they play an important role in the useful life of NBR15.575 buildings (ABNT 2013). They can also contribute to a greater thermal comfort considering that ceramic tiles can provide an additional barrier to the passage of heat. Its use and application are complex and require special care. Errors in the choice of materials or in the execution of the construction system may result in undesirable failures that compromise its role in the context of building comfort. In general, tests that damage the site and present high variability in results can identify changes in ceramic tiles (Takeda; Mazer, 2018). However, there are non-destructive techniques. Among them, infrared thermography (IRT) stands out. It has been increasingly used for facade inspection (Grinzato 2011; Kyliliet al. 2014).

However, there are few studies on the thermal performance of facades, especially using IRT(Kirimtat;Krejcar 2018). Infrared thermography is a non-destructive test technique that allows evaluating temperature distribution patterns based on the heat emitted by the material's surface. IRT can be performed by an active or passive method, obtaining qualitative and quantitative results (Meola, 2018). In the passive method, the stimulus occurs due to an environmental solar charge acting on the building. In this case, there must be a natural temperature difference between the object and the medium where it is (Edis, Flores-Colen, Brito, 2014; Arndt, 2010; Barreira, Almeida, Moreira, 2017). In the active method, a heat or cooling stimulus is necessary to cause a temperature change on the material surface(Gu, Unjoh, Naito 2020; Lerma, Barreira, Almeida, 2018; Francois et al. 2020; Castellini, et al.,2020). Because it is a non-contact investigation technique, IR has been used in civil engineering because it has advantages over other measurement methods.

The advantages are ease of operation of equipment, measurement speed, obtaining quick responses, and agility in diagnostic processes (Chrzanowski, 2010; Kassu, Farley, Tsoli, 2021). Currently, IRT is effective in finding irregularities in the use and application of materials. Research conducted by Kylili et al. (2014) shows that for building diagnostics, IRT can be used to identify heat/cold leakage, infiltrations, and detachment of ceramic tiles on the facade. Different authors have applied this method to locate cracks, failures of cladding laying, to determine effects of color on ceramics (Lourenço, Matias, Faria, 2017; Bauer, Milhomem, Aidar, 2018; Edis, Flores-Colen; Brito, 2015; Santos, Rocha e Póvoas, 2019), superficial humidity in historic buildings (Valero, et al. 2019), capillarity in masonry (Barreira; Almeida and Delgado, 2016), plastering mortar detachment (Freitas, Carasek, Cascudo, 2014; Bauer et al., 2016), and moisture and porosity of the mortar (Poblete, Pascual, 2007). As for the thermal performance of the building, the analyses are restricted to the detection of heat losses and identification of materials (Ocaña, Guerrero and Requena, 2004; Barreira; Freitas, 2007).

However, it must be emphasized that IRT inspection has its specificities and requires knowledge on the part of the evaluator and some fundamental parameters to obtain reliable answers. In this sense, IRT can be accompanied by complementary tests or be verified by other equipment whenever there is a need to determine precise temperatures. In these cases, it is necessary to determine the emissivity of materials with precision and introduce other parameters in the thermal imager (Crisóstomo; Pitarma, 2019).

According to Usamentiaga et al. (2014), to apply this technique it is necessary to evaluate the fraction of thermal radiation that is reflected and that suffers atmospheric attenuation due to atmosphere transmittance, variation in ambient temperature, and relative air humidity. Despite such different studies, there are still no standardized procedures that consider such variables for a perfect execution of tests (Edis, Flores-Colen; Brito 2014; Lucchi, 2018).

In this study, we used active IRT to evaluate the contribution of cladding as a thermal barrier to the passage of heat in structural masonry prototypes built in ceramic tiles in a controlled, artificially heated environment in order to control variables. Active thermography was chosen because it has a more quantitative character than passive thermography, since one can measure and control parameters such as heat source, time, intensity and distance (Francois, et al., 2020).

MATERIALS AND METHODS

In this study, it was used active IRT to evaluate the thermal performance of models built with structural masonry blocks in red clay. The final cladding was ceramic tiles, and the plates were laid according to the recommendations of NBR 13.755 (ABNT 2017). The stimulation of samples was performed using a thermal box built based on studies by Barbosa et al. (2018). Commercial software it was used an auxiliary tool to investigate the occurrence of convection effects inside the thermal box and establish the heating system and to analyse the temperature profile of the samples during heating.

Materials

The materials used in the manufacturing of samples were a hollow structural block of red clay (0.39 m long, 0.14 m wide, and 0.19 m high), square plates (0.10 m) of satin ceramic, Portland cement CPV-ARI, natural quartz sand (for roughcasting), industrialized multiple-use mortar (for laying blocks), industrialized AC-II adhesive mortar (for laying ceramic tiles), type II ceramic grouting mortar, and potable water. The thermal box (0.48 m wide, 0.70 m long, and 0.49 m high) was built using MDF (0.015 m thick), fixing screws, metal hinges, and pressure latches as a seal.

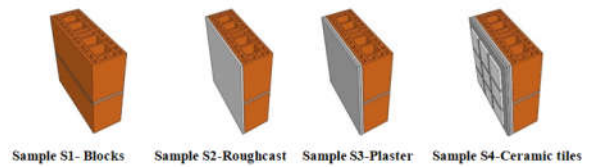


Figure 1. Experimental model, sample assembling



Figure 2. Sample and thermal camera positioned for readings in the thermal box.

The internal part of the box was covered with insulating plates of AT-1260 *Texfiber* (0.0254 m) to avoid heat losses by conduction.

Method

Four samples were prepared according to the design shown in Figure 1. Sample S1 - blocks joined by industrialized mortar; sample S2 - blocks joined by mortar and roughcast (at an 1:3 ratio: one part of cement for three parts of quartz sand); sample S3 - blocks joined by mortar, roughcast, and plaster (at a ratio of 7 kg of mortar to one liter of water); sample S4 - blocks joined by mortar, roughcast, plaster, laying mortar, ceramic tiles laid according to NBR 13755 (ABNT 2017) and the manufacturer's instructions, and flexible grout. It should be noted that the transmittance (U) of each model is different (different thickness and materials), so the comparative study between S1, S2 and S3 evaluates the influence of the different layers. In the case of sample S4, it is expected that the thickness and materials will influence the transmittance and consequently the surface temperature of the material (face opposite to the heat source). After the curing time of the prototype construction steps, each sample was positioned at the front of the thermal box, at a distance of 100mm from the axis of the lamps, and sealed at the top, leaving only one surface in contact with the heat flow and the other face exposed for reading temperature IRT. Preliminary experiments showed that the use of one 1000W halogen lamp located on the center-back of the box promoted non-uniform heating of the sample. In this case, we used four halogen lamp 200W positioned at the back of the box, but evenly distributed. The estimated time to stabilize temperature and for the heat to manifest on the opposite face of the blocks was 30 minutes. The values obtained in the simulation were compared with thermographic images taken of samples. The measurements were performed using active IRT and the heat of halogen lamps as a heating source. The external surface of the samples was monitored by a Flir Systems SC-660 thermographic camera. It has 1% accuracy or $\pm 1^\circ\text{C}$ ($\pm 1^\circ\text{C}$ or $\pm 1\%$ for limited temperature range), and temperature range between -40°C and 1500°C , coupled in a support positioned at 0.90 m of the samples (Figure 2). The heating profile of the different samples was also analyzed, using athermocouple (*Datalogger* from *Agilent*) that measured the temperature at the bottom of the samples (without the influence of convection) every 10 minutes until 60 minutes had elapsed. It was also necessary to determine the emissivity of materials to obtain more precise temperature spectrum and minimize reading errors.

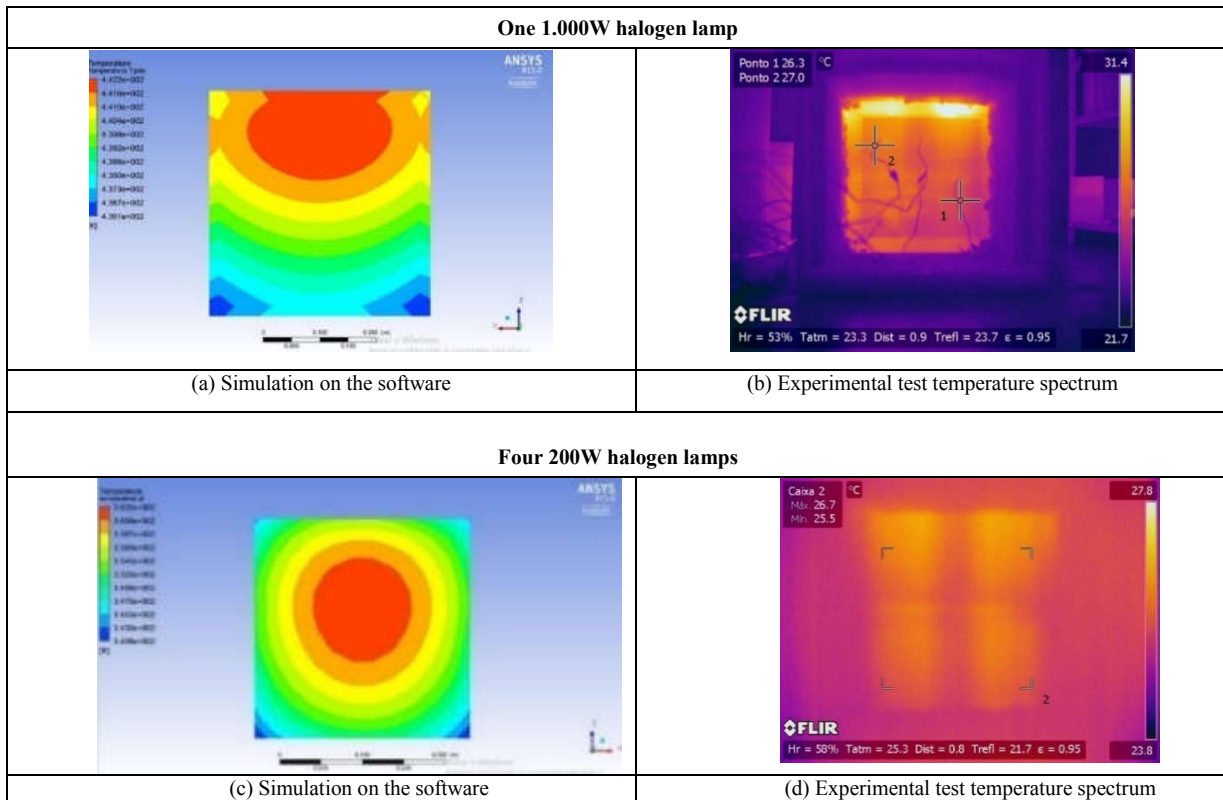


Figure 3. Convection effects using one 1000W lamp and Four 200W lamps

Table 1 - Time taken to stabilize at 25°C, vary the temperature by 2°C, and after 60 minutes of heating

Sample	Start heating T ₁ (min)	Variation 2°C T ₂ (min)	T ₁ - T ₂ (min)	60minutes (°C)
S1 - Block	26	39	13	34.1
S2 - Roughcast	32	45	13	31.6
S3 - Plaster	38	52	14	28.5
S4 - Ceramic Tile	32	56	24	27.9

Table 2. Minimum and maximum temperatures read on profile lines

Sample	Temperature(°C)			Block Rel. (%)
	Minimum	Maximum	Average	
S1 - Block	32.2	34.1	33.1	0.0
S2 - Roughcast	29.0	30.5	29.7	1.4
S3 - Plaster	26.3	27.8	27.0	6.1
S4 - Ceramic tiles	25.3	26.5	25.9	7.2

A small variation in emissivity can cause a considerable change in the detected temperature value (Vishnevetsky, *et al.* 2019). It used the known temperature technique obtained in the material and the values were compared with the different emissivity values shown in the camera display until a value corresponding to the temperature read by the thermocouple was reached. The emissivity values found were 0.95 for the samples S1, S2 and S3 (Crisóstomo, Pitarma, 2019; Avdelidisa, Moropoulou, 2003), and the value for samples coated with ceramic was 0.92. This difference is due to the satin surface of the ceramic tile (Barreira, Almeida, Simões, 2021). Active IRT tests were carried out in laboratory on alternate days so that the thermal box and the samples were in equilibrium with the environment. For control, reflected temperature, room temperature, and relative air humidity were measured using a Testo 622 thermo hygrometer. The recorded average temperature was 25.3 °C, the reflected temperature was 21.7 °C, and the relative air humidity was fixed at 58%. The thermographic equipment was adjusted with these inputs and the distance to the sample (0.80 m). To monitor the surface temperature of samples, readings were taken 60 minutes after heating along profile lines drawn at the bottom of the blocks. Data were analyzed using the software *Therma CAM Quick Report*.

RESULTS AND DISCUSSION

Study of heat propagation: Figure 3 shows the results of simulations made by the software de finite element and the thermographic test carried out on the sample. The result (Figure 3a) of the simulation using with one halogen lamp (1000W) for heating shows that there was a concentration of heat in the upper part of the sample and the thermography obtained similar results (Figure 3b). It's important to note that in the simulation (Figure 3c) with four halogen lamps (200W), there is an attenuation of heat, which concentrated in the central part of the sample and indicated a better distribution of heat inside the thermal box. Thus, for the other experiments, four lamps were used as a heat source. The thermographic readings were taken at the bottom of the sample, where the convection effect was attenuated (Figure 3d).

Determination of the heating profile: Active IRT allows visualizing changes in different materials through a set of images and thermal data. Although the analysis is in general simple and even intuitive (knowing the object under analysis), it is important to prove its real capabilities with real data at this stage of the study.

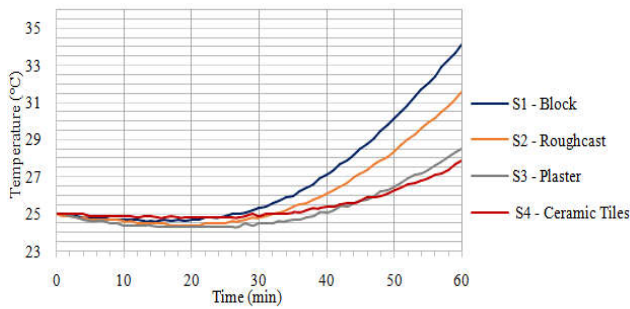


Figure 4. Average temperature profile of the samples over time

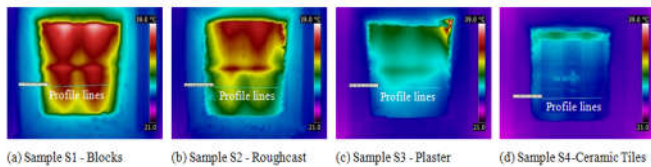


Figure 5. Temperature spectrum of the samples 60 minutes after heating in the thermal box

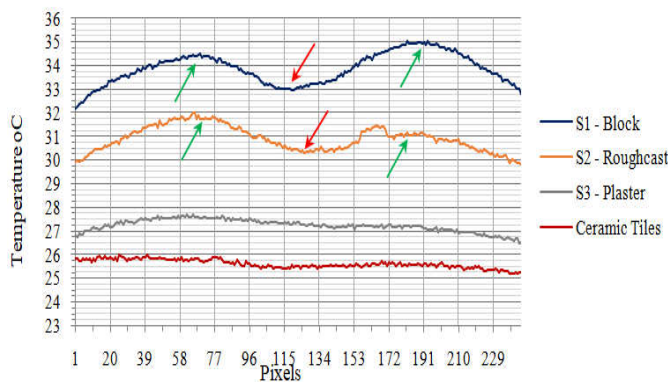


Figure 6. Temperature profile of samples

Thus, it is expected that materials have a certain resistance to heat conduction at the initial phase of tests because construction materials have a high thermal inertia, that is, the capacity to store heat (Grinzato, *et al.*, 2011). Figure 4 shows that, for the materials under study, this resistance lasted from 25 to 38 minutes. Models consisted of more layers presented a longer resistance time (Incropera, Dewitt, 2014). The behavior from then on differed for samples. Table 1 shows the times required for each sample to vary 2°C on the opposite surface and the maximum temperature values after 60 minutes of heating. On analyze the slight temperature decrease observed at the initial phases of the heating might be interesting and beneficial. Samples S1 took 26 minutes to start heating, followed by samples S2 and S4, which took 32 minutes; samples S3 took the longest time 38 minutes. Taking into account the time that each sample takes to increase its surface temperature by 2°C, the results indicate that samples S1, S2 and S3 took practically the same time to vary 2°C (13 and 14 minutes), while S4 took 24 minutes. The analysis of the maximum temperatures reached at 60 minutes allows to identify the influence of the number of layers of the material applied. The highest temperatures were recorded for samples S1 and S2 (34.1 and 31.6°C, respectively), probably because they have less mass. The other samples reached similar temperatures (between 27.7 and 28.5°C), showing that the differences were subtle and within the measurement error of $\pm 2^\circ\text{C}$. The results show that ceramics play an important role in the thermal performance of the façade, and probably in the thermal comfort of the building which requires other parameters to be considered.

Determination of temperature profiles: Figure 5 shows the temperature spectrum and profile lines for each sample. The differences are easily detectable by the color scale. The scale of the

temperature spectrum has been set to 39 and 21°C, in order to be able to compare and take into account the laboratory temperature. As shown by the graduated color bar on the left side of the thermogram. The reddish areas correspond to the highest temperatures, and the purple areas correspond to the lowest temperatures. From qualitative analysis, it is possible to identify the convection effects in the upper part of all samples, even when using four halogen lamps of 200 W. Probably due to the longer exposure time. The applied materials influenced the surface temperature. The geometry of blocks is perceived by the structural divisions in the samples S1 and S2 (Figure 5a and 5b). It promoted an accumulation of thermal energy in empty spaces, which resulted in an increase in temperature. However, the heat was transmitted more slowly where there were divisions. In sample S3 (Figure 5c), the presence of the plaster caused a greater resistance to the passage of heat through the material. The reference sample S4 (Figure 5d) shows a uniform temperature behavior on the sample surface. However, to prove the differences analytically, it was performed a more detailed survey of temperatures using the same software.

Profile lines were drawn to identify the temperatures along a direction and thus calculate the temperatures for further analysis. In the case under study, horizontal lines were drawn on the underside of the sample in order to avoid the influence of convection. To assist in the analysis and treatment of the data the *Therma CAM Quick Report* software was used to capture all the points contained in the profile line drawn on the underside of the samples and to check the values outside the convection area. The graph in Figure 6 shows the temperature values for all points read along the profile lines. The curves obtained by the identifying the internal structure of the ceramic blocks (voids) of the samples S1 and S2 expressed by the sinuous line in the graph shows higher temperatures in this region, this is due to the accumulation of energy in these spaces (green arrows). However, in the areas where there was bonding mortar the heat was transmitted more slowly (red arrow). In the other samples, this effect is mitigated due to the materials introduced in the sample surfaces, evidencing lower temperatures that are uniform in the other samples. These variations are due to the influence of the voids (air present) and the different materials, which influence the heat transmission through the blocks, once the heat source has been kept constant. The behavior of temperatures follows those identified in previous analyses, that is, the tendency is that the samples that received the ceramics present subtle differences more difficult to be identified. However, more quantitative values can be determined.

Table 2 shows the minimum, maximum, and average temperatures read along the profile lines. As expected, the materials applied to the surface of the samples influence the temperature read in the temperature spectrum when compared to previous analyses. It is clear that they are lower depending on where the profile line was drawn. However, in the samples S1, S2 and S3 the average temperatures are the highest (33.1, 29.7 and 27.0°C), while in the sample that received the ceramic coating the temperature was the lowest 25.9°C in sample. Importantly, the ceramic played an important role in retaining the heat flow through the material. This indicates that facades clad with ceramic tiles can retain the heat better compared to facades with ceramic block, roughcast and plaster. Consequently, the ceramic tiles retain heat for longer, preventing it from passing into the room, generating better comfort inside the building.

CONCLUSION

The results show that active IRT has a great potential for model analysis and that the choice of materials and the way to handle them during construction can influence the thermal comfort of the building. The software of finite element makes it possible to identify the effects of convection and that 200W lamps produce a better distribution of heat inside the thermal box. Consequently, it allows identifying the best place to collect sample quantitative data in profile lines. The ceramic played an important role in retaining the heat flow through the material. This indicates that facades clad with ceramic tiles can retain the heat better compared to facades with ceramic block,

roughcast and plaster. Consequently, the ceramic tiles retain heat for longer, preventing it from passing into the environment, generating better comfort inside the building.

AGRADECIMENTOS

FAPEMIG (Foundation for the Support of Minas Gerais State Survey), Brazil, to CAPES (Coordination for the Improvement of Higher Education Personnel), Brazil, to CNPq (Council National Scientific and Technological Development), Brazil, for supporting the study.

REFERENCES

- Arndt, R. W. (2010) Square pulse thermography in frequency domain as adaptation of pulsed phase thermography for qualitative and quantitative applications in cultural heritage and civil engineering. *InfraredPhysicsTechnol.* p.246-253, <https://doi.org/10.1016/j.infrared.2010.03.002>
- Associação Brasileira de Normas Técnicas (ABNT) – NBR 13755: Revestimentos cerâmicos de fachadas e paredes externas com utilização de argamassa colante - Projeto, execução, inspeção e aceitação – Procedimento. Rio de Janeiro: ABNT, 2017.
- Associação Brasileira de Normas Técnicas (ABNT) NBR 15.575: Edificações Habitacionais – Desempenho – Parte 4: Requisitos para os Sistemas de Vedações Verticais internas e externas. Rio de Janeiro: 2013.
- Avdelidisa, N.P. Moropoulou, A. (2003) Emissivity considerations in building thermography. *Energy and Buildings* v. 35 663–667. [https://doi.org/10.1016/S0378-7788\(02\)00210-4](https://doi.org/10.1016/S0378-7788(02)00210-4)
- Barbosa, P.G.; Rodrigues, C.; Alvarenga, C. B. C. S.; Andrade R. M.; Aguiar M. T. P.; Sales, R. B. C. (2018) Evaluation of thermal diffusivity in ceramic blocks using infrared thermography. *International Journal of Engineering Technology Research & Management*. Vol 01, Issue (12) ISSN: 2456-9348.
- Barreira, E.; Almeida, R. M.S.F.; Moreira M. (2017) An infrared thermography passive approach to assess the effect of leakage points in buildings. *Energy and Buildings* 140 p. 224–235. <https://doi.org/10.1016/j.enbuild.2017.02.009>
- Barreira, E.; Almeida, R.M.S.F.; Delgado, J.M.P.Q. (2016) Infrared thermography for assessing moisture related phenomena in building components. *Construction and Building Materials*. V.110, pp. 251–269, <https://doi.org/10.1016/j.conbuildmat.2016.02.026>.
- Barreira, E.; Almeida, R.M.S.F.; Simões, M.L. (2021) Emissivity of Building Materials for Infrared Measurements. *Sensors*, 21, 1961. <https://doi.org/10.3390/s21061961>.
- Barreira, E.; Freitas, V. P. (2007) Evaluation of Building Materials Using Infrared Thermography. *Construction and Building Materials* v. 21, n. 1, pp. 218-224 <https://doi.org/10.1016/j.conbuildmat.2005.06.049>
- Bauer, E. Milhomem, P. M. Aida L. A. G. (2018) Evaluating the damage degree of cracking in facades using infrared thermography. *Journal of Civil Structural Health Monitoring* 8: 517–528. [https://doi.org/10.1007/s13349-018-0289-0\(0123456789](https://doi.org/10.1007/s13349-018-0289-0(0123456789)
- Bauer, E.; Pavón, E.; Barreira, E.; Decastro, E. K. (2016) Analysis of building facade defects using infrared thermography: Laboratory studies. *Journal of Building Engineering*, pp. 93–104. <https://doi.org/10.1016/j.job.2016.02.012>
- Castellini, P; Martarelli, M; D’Antuono, A; Paone N. (2020) Soft-sensing reconstruction of in-depth defect geometry from active IR-thermography data. *Measurement Science and Technology*. Volume 31, Number 12. <https://doi.org/10.1088/1361-6501/aba886>
- Chrzanowski, K. (2010) *Testing Thermal Imagers - Practical Guide*. Military University of Technology. Warsaw, Polônia.
- Crisóstomo, J; Pitarna, J. C. R. (2019) The Importance of Emissivity on Monitoring and Conservation of Wooden Structures Using Infrared Thermography. *Advances in Structural Health Monitoring*. <http://dx.doi.org/10.5772/intechopen.82847>
- Edis, E., Flores-Colen, I., Brito, J. (2014) Passive thermographic detection of moisture problems in façades with adhered ceramic cladding. *Construction and Building Materials* V. 51, pp 187-197. <https://doi.org/10.1016/j.conbuildmat.2013.10.085>
- Edis, E., Flores-Colen, I., Brito, J. (2015) Quasi-quantitative infrared thermographic detection of moisture variation in facades with adhered ceramic cladding using principal component analysis. *Building and Environment*, v. 94 pp. 97-108. <https://doi.org/10.1016/j.buildenv.2015.07.027>
- Francois, A.; Ibos, L.; Feuillet, V.; Meulemans, J. (2020) In situ measurement method for the quantification of the thermal transmittance of a non-homogeneous wall or a thermal bridge using an inverse technique and active infrared thermography. *Energy and Buildings*. <https://doi.org/10.1016/j.enbuild.2020.110633>
- Freitas, J. G. de; Carasek, H.; Cascudo, O. (2014) Utilização de termografia infravermelha para avaliação de fissuras em fachadas com revestimento de argamassa e pintura. *Ambiente Construído*, Porto Alegre, v. 14, n. 1, p. 57-73, jan./mar. <https://doi.org/10.1590/S1678-86212014000100006>
- Grinzato, E.; Cadelano, G.; Ludwig, N.; Bertucci, M. (2011) Infrared thermography for moisture detection: a laboratory study and in-situ test. *Materials Evaluation*, v. 69, n. 1, p. 97-104.
- Gu, J.-C.; Unjoh, S.; Naito, H. (2020). Detectability of delamination regions using infrared thermography in concrete members strengthened by CFRP jacketing. *Composite Structures*, 245, 112328. doi: 10.1016/j.compstruct.2020.112328 url to share this paper: <https://doi.org/10.1016/j.compstruct.2020.112328>
- Incropera, F.P.; Dewitt, D.P. (2014) *Fundamentos de Transferência de Calor e Massa*. 7 ed. LTC. Rio de Janeiro.
- Kassu, A.; Farley III, C.; Tsoli, C. (2021) Laser Heating and Infrared Thermography of Building Materials. *Journal of Building Construction and Planning Research*, 9, 223-229. <https://doi.org/10.4236/jbcpr.2021.93014>
- Kirimat, A; Krejcar O. (2018) A review of infrared thermography for the investigation of building envelopes: Advances and prospects. *Energy and Buildings*, v. 176 390–406. <https://doi.org/10.1016/j.enbuild.2018.07.052>
- Kylili, A.; Christou, P.; Fokaides, P.; Kalogirou S. A. (2014) Infrared thermography (IRT) applications for building diagnostics: A review. *Applied Energy*, v. 134: 531-549. <https://doi.org/10.1016/j.apenergy.2014.08.005>
- Lerma E.; C.; Barreira, E.; Almeida, R. (2018) A discussion concerning active infrared thermography in the evaluation of buildings air infiltration. *Energy and Buildings*. 168:56-66. <https://doi.org/10.1016/j.enbuild.2018.02.050>
- Lourenço, T.; Matias, L.; Faria, P. (2017) Anomalies Detection in Adhesive Wall Tiling Systems by Infrared Thermography. *Construction and Building Materials*, v. 148, p. 419-428. <https://doi.org/10.1016/j.conbuildmat.2017.05.052>
- Lucchi, E. (2018) Applications of the infrared thermography in the energy audit of buildings: A review. *Renewable and Sustainable Energy Reviews* v. 82, 3077–3090. <https://doi.org/10.1016/j.rser.2017.10.031>
- Meola, C. (2018) *Infrared Thermography Recent Advances and Future Trends*. Bentham Science Publishers. 249 pages. <https://doi.org/10.2174/9781608051434112010>
- Ocaña, S.M. Guerrero, I.C. Requena, I.G. (2004) Thermographic survey of two rural buildings in Spain. *Energy Build.* v. 36, 515–523. <https://doi.org/10.1016/j.enbuild.2003.12.012>
- Poblete A, Pascual MA. (2007) Thermographic measurement of the effect of humidity in mortar porosity. *InfraredPhysTechnol.* <https://doi.org/10.1016/j.infrared.2006.06.009>
- Santos, C. F.; Rocha, J. H. A.; Póvoas, Y. V. (2019) Utilização da termografia infravermelha para detecção de focos de umidade em paredes internas de edificações. *Ambiente Construído*, v. 19, n. 1, p. 105-127. <http://dx.doi.org/10.1590/s1678-86212019000100296>
- Takeda, O. T.; Mazer, W. (2018) Potential of thermographic analysis to evaluate pathological manifestations in façade cladding systems. *Revista de la Asociación Latinoamericana de Control de Calidad, Patología y Recuperación de la Construcción*, vol. 8, no. 1, DOI: <https://doi.org/10.21041/ra.v8i1.181>

Usamentiaga, R., Venegas, P., Guerediaga, J., Vega, L., Molleda J., Bulnes F. G. (2014) Infrared thermography for temperature measurement and non-destructive testing. *Sensors (Basel)*, v.14, pp. 12305-12348. <https://doi.org/10.3390/s140712305>

Valero, L.R., Sasso, V. F., Prieto, E.; Vicioso, P. (2019) In situ assessment of superficial moisture condition in façades of historic building using non-destructive techniques. *Case Studies in Construction Materials*, <https://doi.org/10.1016/j.cscm.2019.e00228>

Vishnevetsky, I.; Rotenberg, E.; Kribus, A.; Yakir, D. (2019). Method for accurate measurement of infrared emissivity for opaque low-reflectance materials. *Applied Optics*. v. 58. <https://doi.org/10.1364/AO.58.004599>
